

Review

# Thermal Transformation of Secondary Resources of Carbon-Rich Wastes into Valuable Industrial Applications

Sepideh Hemati , Sanjith Udayakumar, Charlotte Wesley, Smitirupa Biswal, Md. Shahruc Nur-A-Tomal ,  
Negin Sarmadi, Farshid Pahlevani \*  and Veena Sahajwalla

Centre for Sustainable Materials Research and Technology (SMaRT@UNSW), School of Materials Science and Engineering, UNSW, Sydney, NSW 2052, Australia

\* Correspondence: f.pahlevani@unsw.edu.au; Tel.: +61-(2)-9065-7750

**Abstract:** Carbon-based materials have become an indispensable component in a myriad of domestic and industrial applications. Most of the carbon-based end-of-life products discussed in this review end up in landfills. Where recycling is available, it usually involves the production of lower-value products. The allotropic nature of carbon has been analysed to identify novel materials that could be obtained from used products, which also transform into a secondary carbon resource. Thermal transformation of carbon-rich wastes is a promising and viable pathway for adding value to waste that would otherwise go to landfills. The valorisation routes of four different carbon-rich wastes by thermal transformation are reviewed in the study—automotive shredder residue (ASR), textile wastes, leather wastes, and spent coffee grounds (SCGs). Textile wastes were thermally transformed into carbon fibres and activated carbon, while ASRs were used as a reductant to produce silicon carbide (SiC) from waste glass. The leather wastes and spent coffee grounds (SCGs) were employed as reductants in the reduction of hematite. This paper examines the possible routes of thermally transforming carbon-rich wastes into different industrial processes and applications. The transformation products were characterised using several techniques to assess their suitability for their respective applications. The strategy of valorising the wastes by thermal transformation has successfully prevented those wastes from ending up in landfills.

**Keywords:** automotive shredder residue (ASR); glass waste; textile waste; spent coffee grounds (SCG); leather wastes; waste valorisation; thermal transformation



**Citation:** Hemati, S.; Udayakumar, S.; Wesley, C.; Biswal, S.; Nur-A-Tomal, M.S.; Sarmadi, N.; Pahlevani, F.; Sahajwalla, V. Thermal Transformation of Secondary Resources of Carbon-Rich Wastes into Valuable Industrial Applications. *J. Compos. Sci.* **2023**, *7*, 8. <https://doi.org/10.3390/jcs7010008>

Academic Editor: Francesco Tornabene

Received: 28 November 2022

Revised: 9 December 2022

Accepted: 19 December 2022

Published: 3 January 2023



**Copyright:** © 2023 by the authors. Licensee MDPI, Basel, Switzerland. This article is an open access article distributed under the terms and conditions of the Creative Commons Attribution (CC BY) license (<https://creativecommons.org/licenses/by/4.0/>).

## 1. Introduction

Rapid urbanisation and socio-economic development throughout the developing and developed countries in the world has ensued a precipitous increase in the generation of municipal, industrial, and agricultural wastes. A typical company value chain includes the extraction of raw materials from international sources, transportation, processing, manufacturing, and packaging into completed products, distribution, and product support, all of which result in the production of a wide variety of wastes. The wastes are generated through various market channels, consumer use of products, and final disposal or recycling of the residuals. These wastes are produced in solid, liquid, and gaseous forms and may contain harmful pollutants and glasshouse gases (GHGs) from fuel burning and improper waste disposal [1]. Recycling and composting programmes are failing to keep up with waste accumulation, even though various firms and non-governmental organisations (NGOs) are developing and promoting novel solutions ranging from high-tech waste processing to enhanced guidance and assistance for waste management communities. The best opportunity for human civilisations to actually lessen the carbon footprint and advance toward a sustainable waste management ecosystem is to expedite the repurposing of waste materials into marketable raw materials for new goods.

The piling up of landfills in the name of waste management does not contribute to a sustainable environment based on a circular economy. A circular economy is one that

keeps the usefulness of materials in the economic system for as long as feasible, decreasing the dependency on natural resources and avoiding the scenario of raw material scarcity and the environmental implications of material consumption and waste disposal. Finding a solution to the dilemma of where and how to dispose of the vast volume of waste produced daily is one of the world's most pressing concerns, especially given that the volume of waste produced is rising. Different recycling techniques and strategies have been proposed to tackle these environmental issues, such as mechanical, chemical, and hybrid methods. Although these methods boast of individually different extents of applications, advantages, and disadvantages, they have built a framework for clean and cheaper ways of reusing end-of-life products.

The burgeoning concerns over solid waste disposal have indeed promoted research efforts dealing with their valorisation routes. In order to minimise metal and non-metallic wastes ending up in landfills, several valorisation alternatives have been proposed, which range from primary routes of direct recycling to quaternary or multi-step routes of waste valorisation. There has been a surge in demand for raw materials and a risk associated with their supply. The geopolitical challenges and technological complexities involved in acquiring raw materials have spawned an interest in recycling the elements from secondary resources. Recycling plastics and polymer-based products have been prevalent for the last few decades. While an enormous and escalating volume of waste from the ubiquitous plastics of different polymer groups is a threat to the environment and life on earth, they are also considered alternative supply chains for a wide range of products and processes. Generally, polymer-based wastes are recycled, downcycled to a different product with lesser value, or disposed into landfills. The diverse attributes of plastics, namely their light weight, strength, heat resistance, high convenience, and low cost, make them versatile for business and consumer uses. However, these materials are high molecular weight organic polymers composed of elements, such as carbon, hydrogen, oxygen, nitrogen, and sulphur. Despite their attractive hydrocarbon composition, their potential as a secondary carbon resource has been underestimated. Contrastingly, incineration or high-temperature pyrolysis of polymer wastes is an efficient method of managing waste, yet comparatively and energy-intensive, involving higher operating costs and greater levels of pollution, and they could harm the environment. Thus far, only a few researchers have attempted to exploit polymer materials, namely polypropylene (PP), polycarbonate (PC), acrylonitrile butadiene styrene (ABS), polyethylene (PE), and polyurethane (PU), as a secondary source of carbon in the material and metallurgical industries. Different polymer groups possess different carbon-hydrogen compositions, and they determine the extent of their utilisation in the subsequent recycling processes [2].

Industrialisation and increasing use of private transport are increasing the production and use of motor vehicles. The automobile sector is one of the dominant consumers of polymeric materials for their interiors, body, and upholsteries. Automotive shredder residue, a heterogeneous mixture of all the materials found in cars, ovens, etc., is produced when ELVs and other scrap are shredded into pieces the size of an orange, and the metal chunks (70%) removed from the rest, usually with an air cyclone, or using magnetic and eddy current separation, for steel recycling [3]. Several researchers have demonstrated the characteristics of ASR because of the presence of a substantial amount of wood and plastic [4].

There are plenty of non-conventional secondary resources of carbon, which are also largely disposed into landfills, i.e., textile and leather wastes. The post-consumer wastes include clothing and other smaller sources, such as furniture, carpets, and footwear. Any type of textile waste can be classified into three main groups: cellulose, protein, and synthetic fibres. Most textile recycling involves a downcycling process, wherein the product made from the recycled material is of lower quality or value than the original product. Interestingly, resource recovery from textile wastes can provide significant environmental and economic gains by replacing products from primary resources. Thermal transformation of textile wastes has been barely paid attention to in the recycling communities, while it has

great potential to be invested as an industry [5]. Leather wastes are another prospective area that has witnessed relatively less progress in terms of recycling. Most leather goods, such as footwear, bags, clothing and furniture, upholstery, and interior design, are downcycled, or closed-loop recycled [6]. However, most of the leather wastes end up in landfills and are incinerated for no benefit. Similar to textile wastes, ‘post-consumer use’ leather products are a rich source of carbon fibers, which have the ability to serve assorted applications [7]. The fibre-based wastes have the tendency to exhibit an upgraded behaviour on undergoing appropriate thermal modification and valorisation processes.

One of the other underutilised materials, yet a rich source of carbon, dumped into the general waste is spent coffee grounds (SCGs). Despite their highly desirable chemical constituents, the SCGs are limited to composting, domestic fertiliser manufacturing processes, and bio-active compounds. Recent decades have realised the potential of these materials in bio-energy applications, material processing, and nutraceuticals [8]. Researchers have recently suggested the possible use of SCGs as a promising source of carbon in metallurgical processes, i.e., iron and steel making. Thermal transformation of these materials has proven the capacity of SCGs as a reductant replacing conventional metallurgical coke and coal [9].

The viability of recycling solutions is constrained by commercial forces, including the strength of end markets, revenue from profit sales, and the cost of recycling operations. Most recycling enterprises seek to be profitable, which adds another cost to the process, and therefore, any product generated from the waste cotton textiles need to be of sufficient value to offset all these costs. In this paper, different secondary carbon sources have been identified, and their potential in different applications after appropriate thermal treatment methods has been elucidated. The material characteristics of the treated products were proposed for various applications based on their intrinsic properties. Textile wastes were transformed into activated carbon, while the ASRs, leather wastes, and SCGs were evaluated as a reductant in metallurgical processes.

## 2. Waste Products: Secondary Resources of Carbon

Four different groups of wastes were focused on as secondary carbon sources, namely used uniform clothing (cotton textile wastes), pre- and post-consumer use leather wastes, automotive shredder residues (ASRs), and Spent Coffee Grounds (SCGs). The current review converges on innovative technologies to uncover high-quality recycled materials, often from unexpected or underutilised sources. A pictorial representation of how different secondary carbon resources disposed into landfills are valorised in the processes of producing value-added industrial materials is presented in Figure 1.

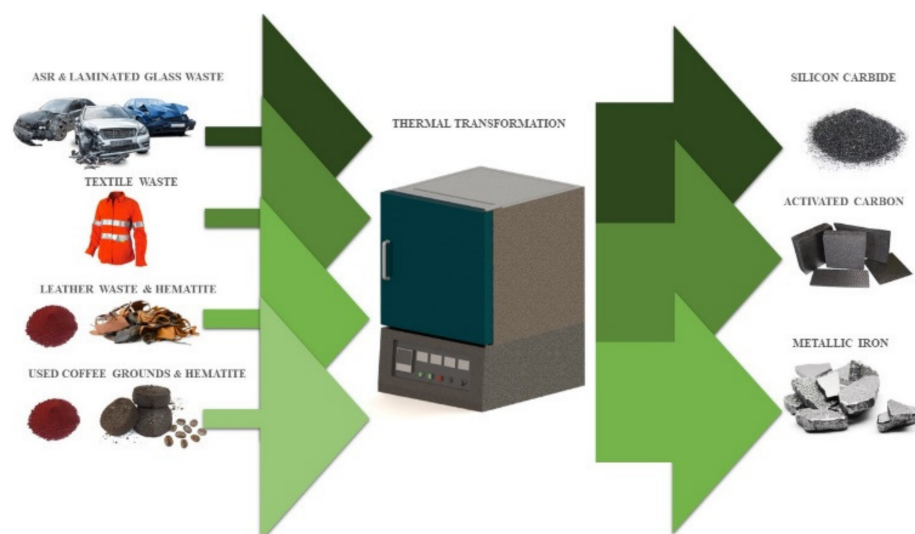


**Figure 1.** Thermal transformation of secondary resources of carbon (wastes).

### 2.1. Textile Waste—Source of Activated Carbon

Cotton is one of the most commonly used materials in the textiles industry, either as pure cotton or in a blend with other fibres [10]. One of the more prominent is ‘polycotton’, which typically involves blends of polyester and cotton in ratios of 50:50, 35:65, and 65:35, respectively. The focus of this study is cotton textiles of 100% purity, which are commonly used for clothing and personal protective equipment because of their thermal resistance and strength. Cotton textiles are appealing to consumers because it is ‘breathable’, durable, and low maintenance. The fibres within a cotton plant are almost entirely cellulose, and the stem is lignin [11]. Only cotton fibres are used in cotton textiles, wherein they are separated from the seeds in a process commonly referred to as ‘ginning’. The fibre is then spun into yarn and subjected to dyeing and manufacturing processes to prepare a textile. Being a rich source of cellulose, textile wastes are a promising precursor to activated carbon. There is no best approach to recycling cotton waste textiles. All solutions should be guided by the waste hierarchy. For these reasons, thermal transformation processes to create carbon fibres and activated carbon fibres are considered a commercially viable solution in situations where simpler recycling processes compete with inexpensive primary materials (for example, many consumer cloths or rags used for washing or cleaning are primary materials despite recycled cloths being a better choice for the environment). For higher-value materials, consumers are more likely to be more thoughtful in their choice and look for cost savings where available.

### 2.2. Reductants in Metallurgical Processes

One of the most critical challenges engineers and scientists face to solve is managing the limited resources on our planet and waste material. Australia generated nearly 67 million tonnes of waste in 2016–2017 (2018). Among different industry sectors, the automotive industry is the leading resource-consuming and waste producer [12]. The volume of waste material from end-of-life-vehicle (ELVs) is immense and necessitates applicable management. The end-of-life-vehicle (ELVs) waste management process is classified into three broad stages, including (I) depollution, (II) dismantling, and (III) shredding [13]. The entire shredded output encompasses about 70–75% ferrous fraction and nonferrous metals, as the 20% to 25% residual from shredded production is known as the automotive shredder residue (ASR) [3]. Waste glass is commonly recycled into new glass products, such as bottles and jars, in traditional recycling processes. Industries and researchers use waste glass in the construction sector. However, producing recycled glass products such as waste glass containing plastic and other materials is challenging. For instance, recycling the windscreens and windows of automobiles with laminated and tempered float glass is tricky due to the plastic lamination in the interlayers of the glasses and melting points, which vary from glass-to-glass sources such as waste jars and bottles. Due to the presence of glass, recycling laminated plastic from end-of-life automobiles is likewise cumbersome. Removing the glass impurities from the plastic needs extensive mechanical processing, which is expensive. Additionally, automobile waste containing different glasses types cannot be mixed and is unsuitable for conventional glass recycling procedures. Mostly, ASR is the remaining material after the separation of metals from the shredded materials, which usually contain 19–31% plastic, approximately 20% rubber, 10–42% textile and fibre materials, 2–5% wood residues, and 5.2% glass. Owing to the distinct composition of ASR, they can be used as a reductant source in the thermal transformation of glass wastes.

Tanneries are renowned for being dangerous to the environment and public health. Every year, 6 million tons of solid waste is produced from leather production worldwide [14]. For example, fleshings, splittings, shavings, buffing dust, and leather offcuts are produced in the tanneries. Amongst the most dangerous concerns with leather waste management is the presence of chromium (Cr), which causes a danger to both the environment and human health.  $\text{Cr}^{3+}$  is oxidised to  $\text{Cr}^{6+}$ , which risks a dangerous hazard to humans because of its carcinogenic and mutagenic characteristics [6,15]. A thermal transformation is a novel

way to utilise the potential of leather and tannery wastes as a reducing agent and thereby simultaneously treat them as a harmless product.

One of the most popular beverages in the world is coffee, which is also considered to be one of the most traded products. Around 170 million 60 kg bags of coffee were produced globally, while 165 million 60 kg bags were consumed in the period 2018–2019 [16]. SCGs (spent coffee grounds) are the used coffee grounds frequently left over from the extraction of espresso coffee. According to Planet Ark research, 1 kg of coffee grounds yields around 1.9 kg of SCGs [17]. Since landfills are where most SCGs are disposed of, they release methane gas, which is known to be much more harmful than carbon dioxide. SCGs may contaminate groundwater or water sources close to landfills because they include elements that are detrimental to the environment [18]. Hence, it is necessary to develop technologies that utilise SCGs as feedstock, thus supporting the concept of a circular economy and reducing the inefficient disposal in landfills. The rich carbon content in SCGs suggests their exceptional reducing capability in the production of iron from their ores.

### 3. Thermal Transformation of Different Wastes into Valuable Products

The section discusses the different carbon-based waste utilised in thermal transformation processes for making activated carbon fibres and as a reducing agent in iron ore reduction and production of silicon carbides.

#### 3.1. Textile Wastes

Pure cotton personal protective equipment uniforms were the subject of this investigation because a homogenous supply could be procured for testing, and uniforms are often considered unsuitable for re-use. This is because organisations are often concerned about the possible misuse of company-branded items or uniforms (e.g., police, council, or defence). The complete composition of the uniforms was determined by a combination of chemical analyses, namely X-ray fluorescence (XRF) spectroscopy, CHNS, and oxygen analysis, and inductively coupled plasma mass spectroscopy (ICP-MS) for the major elements. The results show that the sample mostly consists of carbon, oxygen, and hydrogen, with traces of nitrogen, sulphur, silicon, phosphorus, calcium, and iron (Table 1). Elements of similar concentration were determined for other PPE uniforms studied in the literature [19].

**Table 1.** Composition (% by mass) of cotton textile.

Element	O	C	H	S	Ca	N	Others
Mass%	51.11	42.01	6.14	0.21	0.21	0.15	0.17

Upon researching these branded products, it was identified that the pure cotton shirt might have a flame-resistant coating [20]. The nature of this coating could not be determined as it was a ‘trade secret’. This coating could reduce the formation of levoglucosan, which is known to form in the combustion of pyrolytic reactions with cellulose [21]. The presence of the fire-resistant coating is, therefore, an advantage in the prevention of carbon loss during a thermal transformation process [20,22].

#### 3.1.1. Production of Carbon and Activated Carbon Fibres

The first phase of thermal transformation in an inert (argon gas) environment is dehydration. Minimal mass loss occurs before 200 °C, while most of the mass loss occurs between 200 °C and 450 °C and through volatilisation. The pyrolytic products include CO, CO<sub>2</sub>, CH<sub>4</sub>, and C<sub>6</sub>H<sub>10</sub>O<sub>5</sub>. Beyond 450 °C, only carbonisation reactions occur [23]. The activation energy for this reaction was determined to be 138 kJ using the Coats Redfern Method. The chemical analyses of the samples were conducted to determine the temperature and time requirements for desired specifications.

Activated carbon fibres require both chemical and thermal processes to maximise surface area [24]. The textiles were treated with phosphoric acid and distilled water

at variable ratios. The phosphoric opens the pores, so the more acid added, the more degradation and release of O<sub>2</sub>, N<sub>2</sub>, and H<sub>2</sub> gases. With less acid, fewer micropores are formed, and with more acid, more mesopores and macropores are formed. This process occurs over a 24-h period in a low-temperature muffle furnace (i.e., 80 °C). The sample is then transferred to a higher temperature (i.e., 850) in an inert environment (Ar gas). Further dehydration, volatilisation, and carbonisation processes take place during this process. Samples are then washed and analysed using Brunauer-Emmett-Teller (BET) method to measure the surface area [25]. From Figure 2, the lower the amount of acid, the higher the surface area for activated carbon fibres produced from waste cotton textiles.

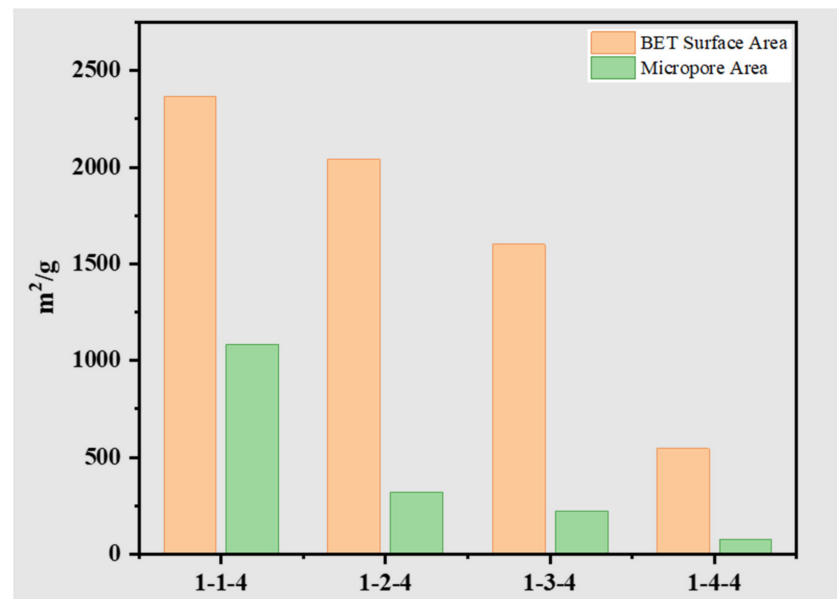


**Figure 2.** Surface area and different textile–phosphoric acid–distilled water ratios (Adapted from Wesley, et al. [25]. Reproduced with permission from Elsevier).

### 3.1.2. Carbon and Activated Carbon Fibres from Waste Cotton Textiles

The relationship between the carbon fibres produced at different temperatures and their carbon contents is presented in Figure 3. The relationship determined the minimum temperature requirements for the desired amount of carbon content in the products. To meet the traditional definition of carbon fibre (90% carbon content), the temperature required for transformation is 1150 °C. The minimum temperature required for a carbon fibre with 80% carbon content was nearly half this at 650 °C. Both products have their own advantages. The former is strong and meets carbon content requirements for applications that require strength and ordered carbon structure. Unlike the former, the latter is relatively soft, not brittle, and retains the textile structure. Carbon fibre markets are growing annually, with emerging markets in the renewable, automotive, and recreation sectors. The flexible and cloth-like structure of the lower carbon content carbon fibre renders it suitable for wearable devices. Jagdale that cotton-derived carbon fibres have superior performance to conventional carbon fibres for energy storage applications [26]. Lower temperature transformations are also preferable from a life cycle perspective. Lifecycle assessments showed that it is better for the environment to use carbon fibres from waste cotton textiles than poly-acrylonitrile, as this traditional precursor is made from petroleum in a non-renewable energy background.

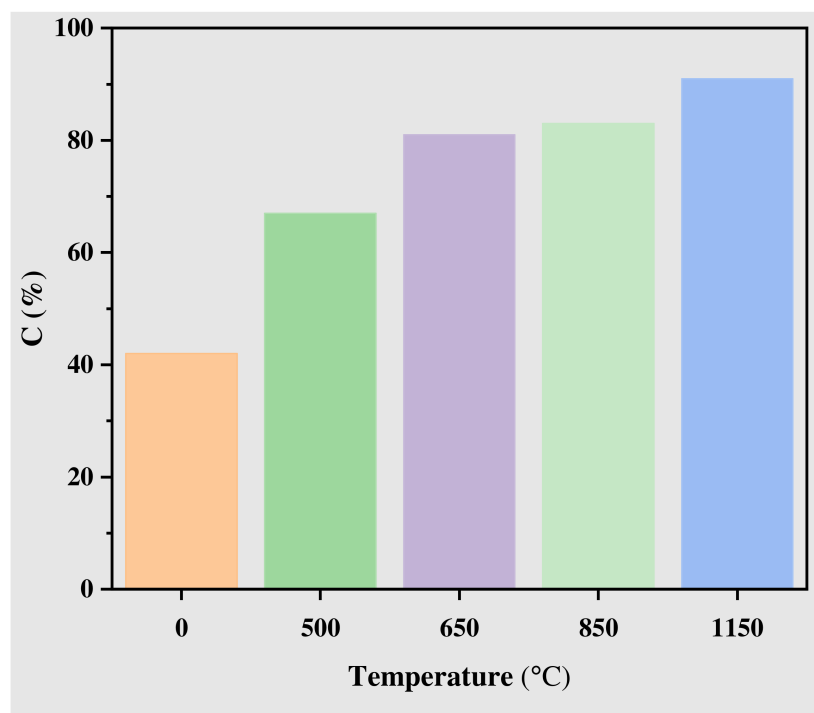


**Figure 3.** Relationship between temperature and carbon content of activated carbon fibres.

Activated carbon fibres need to have a surface area of at least  $1000 \text{ m}^2/\text{g}$  for water treatment applications [27]. For energy storage applications, the surface area must be at least  $1700 \text{ m}^2/\text{g}$  [28]. As shown in Figure 3, the ACFs produced from the waste uniforms exceed these requirements, which are promising for many applications, including emissions control, noise attenuation, and energy storage. The ACFs also retained their cloth structure which is convenient for certain applications such as filter media or noise attenuation panels. Ahammad et al. suggest that ACFs are suitable for use in sensors because of the “large surface area, highly developed porosity, skeletal structural features, and a high degree of surface reactivity” [29]. ACFs are valuable to the industry in a number of contexts, and therefore, there is a strong market pull for this type of recycling process.

### 3.2. Automotive Shredder Residues (ASR) and Glass Wastes

According to studies in the literature, about 27 different sorts of plastics from ASR could be recovered with enough purity. Most plastics are a combination of polypropylene (PP), polyurethane (PUR), polyvinyl chloride (PVC), acrylonitrile butadiene styrene (ABS), poly-methyl-methacrylate (PMMA), and polyethylene terephthalate (i.e., PET) [30–34]. As depicted in Figure 4, various types of plastics are frequently found in automobiles; 44% of the total weight of vehicles was made of polypropylene, which comprises the most plastic type in ASR, around 39%. PP is chemically resistant, has a high tensile modulus and high melting point, a low density, and could be inexpensive; because of this, PP has been leading the share market commodity plastics [35]. Additionally, PP could be enhanced to meet specific requirements without altering its properties [36]. According to Figure 4, the rest of the plastic types mainly in ASR are polyethylene (PE), polycarbonates (PC), and polyurethane (PUR), respectively. There are different methods to recycle plastics. For instance, mechanical sorting is used to refine and sell, thermal treatment, chemical building blocks (feedstock or chemical recycling), heat, or fuel could be obtained [30]. The study employed a selective thermal transformation process by carefully selecting the significant process parameters to produce value-added products from glass wastes and ASRs.

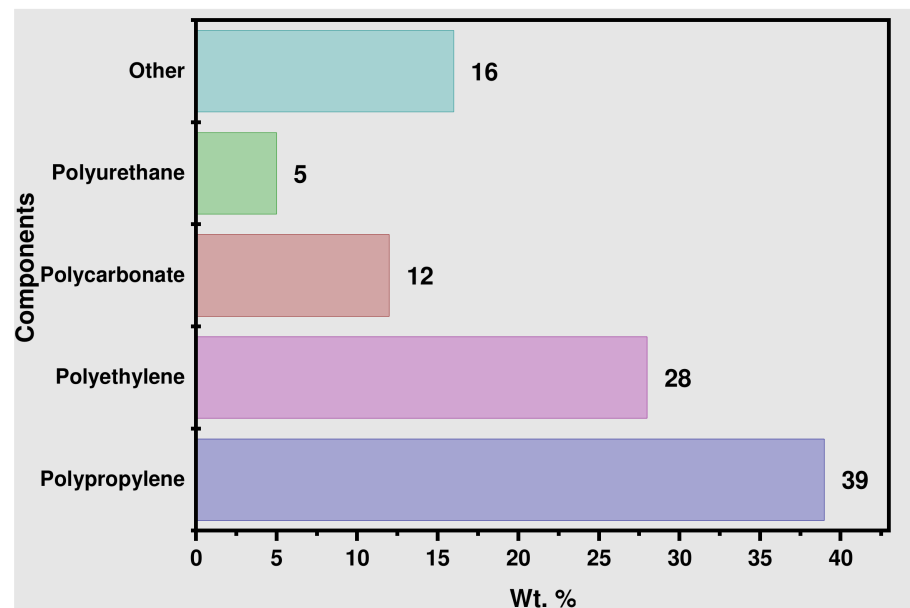


**Figure 4.** Different types of plastics found in ASRs. (Adapted from Hemati, et al. [4]).

### 3.2.1. Thermal Transformation of ASR and Waste Glass

The innovative technology to transform ASR components, which are more likely to decompose into liquids and/or gases using heat, is called the thermo-chemical treatment. The residual solids in the raw ASR materials contain carbonaceous char, mineral ash, and metals [37]. Heat treatment is the emerging technology for the waste and solid plastic waste in thermal and chemical treatment technologies [37–40]. Additionally, it is the most suitable for mixed wastes, including many different plastics blended with other materials, accordingly to ASR streams [41]. In this project, the mixed plastics of ASR and vehicles' windshield glass waste were collected from the Australian regional steel manufacturer. The blended plastic of ASR and the waste glass were shredded separately to get a fine powder. Then they were mixed with weight ratios of 30% waste glass and 70% ASR plastics, and pellets were made via the Carver hot press (Model 2697, Ontario, NY, USA) at 150 °C with a uniaxial pressure (200 bar). Next, the samples were placed in a horizontal tube furnace (Model HTF 7060, Ceramic Engineering, Furnace Manufacturers Sydney, Sydney, Australia) in a high-purity argon atmosphere (>99%, 0.8 L min<sup>-1</sup>) connected to a mass flow controller. The heating chamber temperature was programmed from 700 °C to 1500 °C, and the holding time was 2 h. Then, the as-synthesised materials from the reduction of glass and carbonaceous materials in the furnace chamber were collected and crushed for further analysis.

### 3.2.2. Production of SiC

SiC was produced from waste glass (Si source) obtained from the windshield of automobiles, while ASR plastics were considered the source of carbon. As demonstrated in Figure 5, the formation of SiC began at 1300 °C, and the production of SiC increased with increasing temperature (1500 °C), suggesting that the reaction between Si and C takes place at a higher temperature, as demonstrated by other researchers [42]. From Figure 5, SiC peaks at 1500 °C are more significant than 1300 °C. Conversely, no SiO<sub>2</sub> peaks were observed at 1500 °C; only a minor peak of SiO<sub>x</sub>C<sub>y</sub> was noticed, suggesting the completion of the reaction between the SiO<sub>2</sub> of glass and C of ASR plastics, resulting in total transformation into SiC. SiC peak around 35.69° is the highest, and the SiC at both 1300 °C and 1500 °C has a cubic crystal system [4].

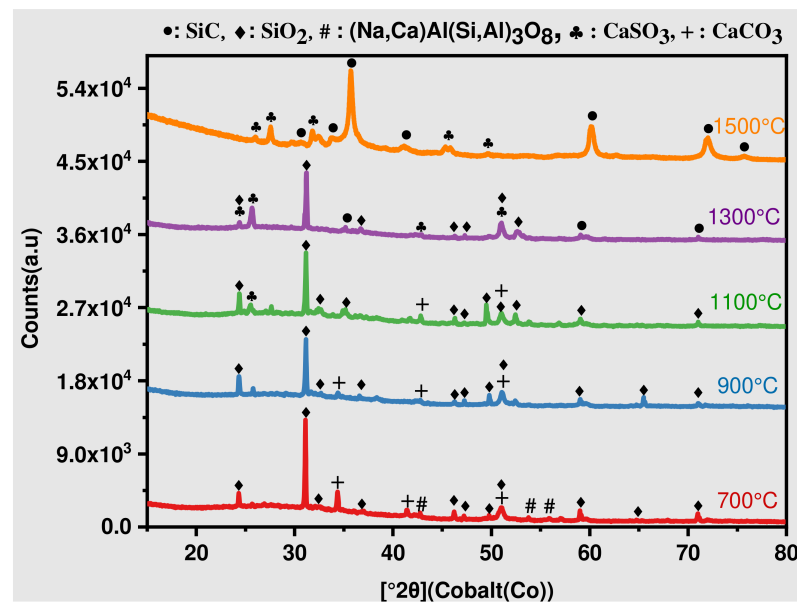


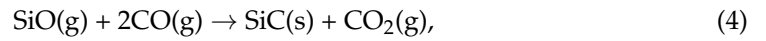
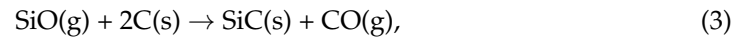
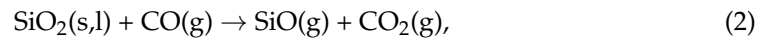
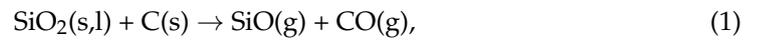
**Figure 5.** XRD spectrums of heat-treated mixed ASR plastics and glass at 700 °C to 1500 °C for 2 h (Adapted from Hemati, et al. [4]).

Transmission electron microscopy (TEM) was used to obtain the structure and morphology of SiC nanoparticles sample from 1500 °C for 2 h of heat treatment. Figure 6a illustrates the low-resolution transmission electron microscopy (LRTEM) image, which shows SiC quasi-spherical particles with a length of fixed edges of nearly 50–100 nm and a porous structure. To form secondary particles with irregular pores, SiC particles are stacked together. High-resolution transmission electron microscopy (HRTEM) plotted in Figure 6b implies that SiC was highly crystallised, meaning that nanoparticles are made of numerous tiny single-crystalline SiC nanoparticles with various orientations. Wang, et al. [43] pointed out that the regularly arranged lattice could determine the high crystallinity of SiC. These perfect diffraction peaks at 35.69°, 60.11°, and 71.78° are related to rings (111), (220), and (311) planes of cubic SiC (Reference code: 00-029-1129) were confirmed by XRD patterns of SiC nanospheres [43]. HRTEM image demonstrates sharp lattice separation of (111) planes with  $d = 0.25$  nm links to the cubic phase of SiC crystals. Referring to Figure 6c, the selected area electric diffraction pattern (SAED) patterns demonstrated nanoparticle is polycrystalline SiC, and each one of the diffraction rings designated to the (111), (220), (311) planes of the cubic SiC, respectively [4].

### 3.2.3. Mechanism of SiC Nanospheres Formation

Heat treatment of plastic of ASR and waste glass helps to produce carbon products and silica layers at a high temperature [4]. The carbothermic reduction of  $\text{SiO}_2$  is the most economical process because of the low-cost raw materials and least reaction equipment to synthesise SiC [31–34]. In synthesising the SiC nanospheres, the reaction temperature and the raw material have substantial roles [35]. The general reaction to produce SiC (6) is the reaction between  $\text{SiO}_2$  with C. Clearly, the formation of SiC is more complicated and requires a sequence of solid-solid, solid-liquid, solid-gas, and gas-gas reactions [36–39]. The synthesis of SiC starts in direct physical contact by reducing  $\text{SiO}_2$  with C (1) [40]. For 2 h, mixed ASR plastics and waste glass were heat treated at 1500 °C.  $\text{SiO}_2$  and C reacted together during heat treatment, and SiO and CO were produced (1). Then, CO with  $\text{SiO}_2$  reacted, forming SiO and  $\text{CO}_2$  (2). The reaction of  $\text{CO}_2$  with the surrounding C creates CO (5), which boosts reaction (4) to produce SiC constantly [37]. Additionally, the reaction of SiO and C could make SiC (3). It can be noted from reaction (4) that the reaction between

SiO and CO together generated SiC. The following reactions illustrated the reduction of SiO<sub>2</sub> with C to synthesise SiC [42,44,45]:



Zibo et al. adopted the common reaction as follows [46]:

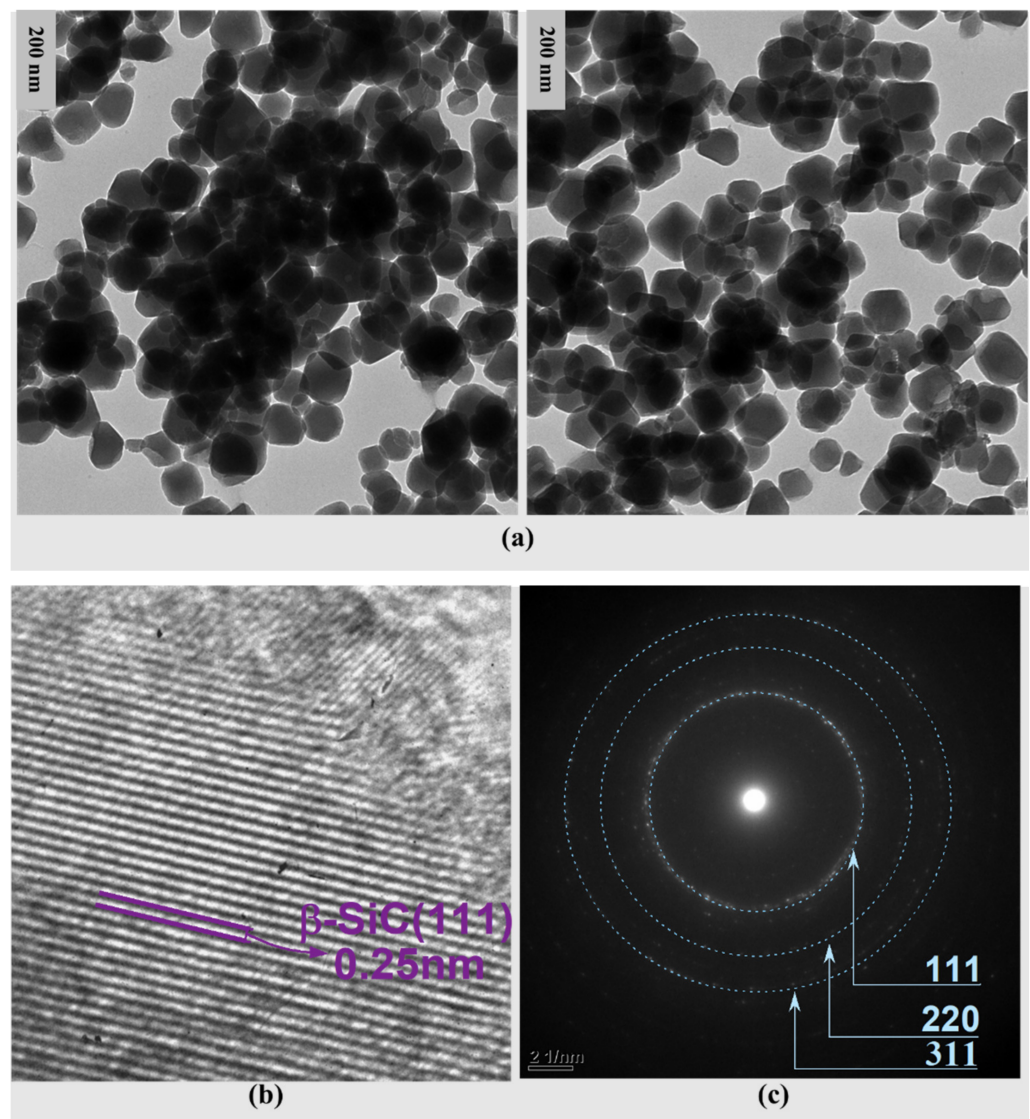


**Figure 6.** (a) A general low-resolution TEM image, (b) a representative high-resolution, (c) a corresponding selected area electron diffraction pattern of SiC nanoparticles obtained at 1400 °C for 1 h (Adapted from Hemati, et al. [4]).

### 3.3. Leather Wastes

Chromium-containing leather wastes have in the study because of their potential carcinogenic effects on improper disposal or treatment. In developing countries, solid wastes are usually landfilled without any treatment, which causes environmental and public health problems [47,48]. Therefore, developing an environmentally sustainable process not only to treat but also utilise these leather wastes is critical.

The pre- and post-consumer use of leather wastes was characterised by numerous analytical tools. The concentration of elements in the samples determined using inductively coupled plasma optical emission spectrometry/mass spectrometry (ICP-OES/MS) is shown in Table 2. The samples have alkali metals, alkaline-earth metals, transition metals, other metals, and some non-metals. A high concentration of Na, Cr, and S is present in the leather wastes.

**Table 2.** The elemental concentration of the chromium-containing leather wastes. All units are in mg/kg. MDL stands for measurement detection limit [7]. \*\* There were insoluble Si in the samples.

Element	MDL	Shavings	Buffing Dust	Leather Cuttings
Cr	5.00	18,114	25,213	8272
Na	50.00	14,194	4549	4625
S	50.00	10,879	17,077	10,801
Mg	5.00	958	809	204
Si **	0.50	49	1983	750
Al	5.00	14.80	3079	39.8
Ca	5.00	686	1252	3766
Fe	5.00	428	530	112
B	0.50	258.0	13.6	3.9
K	5.00	137	228	481
P	5.00	116	619	211
Cu	0.50	0.64	65.6	5.9
Ti	0.50	0.51	56.38	3.65
Ba	0.50	0.43	9.22	27.67
Sr	0.50	5.08	9.25	11.2
Ga	0.50	0.96	2.48	1.81
Ni	0.50	0.97	1.78	1.04
Pb	0.50	0.18	3.45	1.62
Co	0.50	0.19	0.95	0.73

FTIR spectra of the solid leather waste are presented in Figure 7. It is confirmed that the spectra of all samples were almost the same since leather is fabricated from collagen, which is a protein [49]. All the wastes showed peaks at around  $3305\text{ cm}^{-1}$  and  $3075\text{ cm}^{-1}$ , which are assigned to the stretching vibration of N–H in the protein backbone. Besides, all the spectra have distinctive peaks of amide bonds, precisely, a pointed peak at  $1635\text{ cm}^{-1}$  (amide I), a peak at  $1545\text{ cm}^{-1}$  (amide II), and a wide shoulder at  $1030\text{ cm}^{-1}$  (amide III). Additionally, the peak at  $1450\text{ cm}^{-1}$  indicates the stretching vibration of C–C bonds, while the bunch of peaks at  $1450$ ,  $1335$ , and  $1235\text{ cm}^{-1}$  (amide III) correspond to the bending vibration of C–H in the protein [50]. Other researchers have observed comparable functional groups for different leather wastes [51]

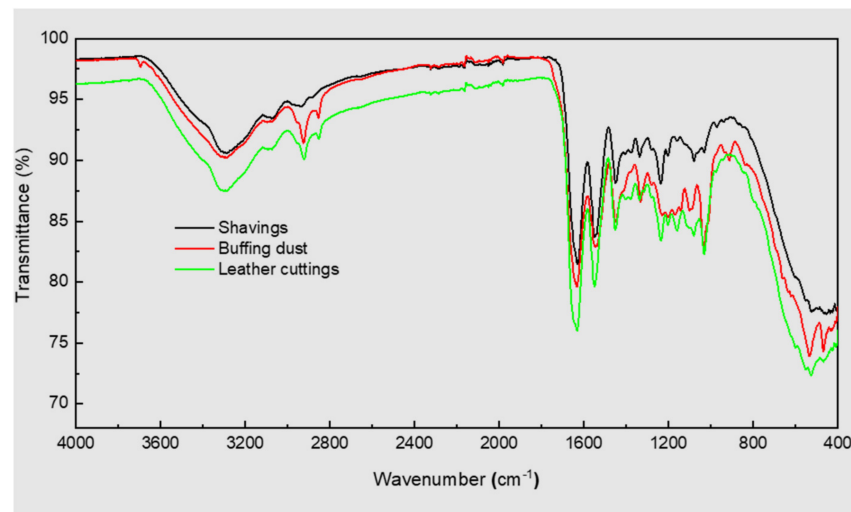


**Figure 7.** FTIR spectra of collected leather wastes (Adapted from Nur-A-Tomal, et al. [7]. Reproduced with permission from Springer Nature).

Thermogravimetric analysis of the samples was reported in Figure 8. It can be seen from the graph that the leather waste samples have three thermal degradation steps [52,53]. The initial weight loss could be a result of the evaporation of absorbed and bound water in the samples, which occurred at around 150 °C. The main loss of weight was observed between 250–600 °C, which could be ascribed to the decomposition of the collagen. Furthermore, the weight loss at 600–800 °C could be due to further pyrolysis of residues [54].

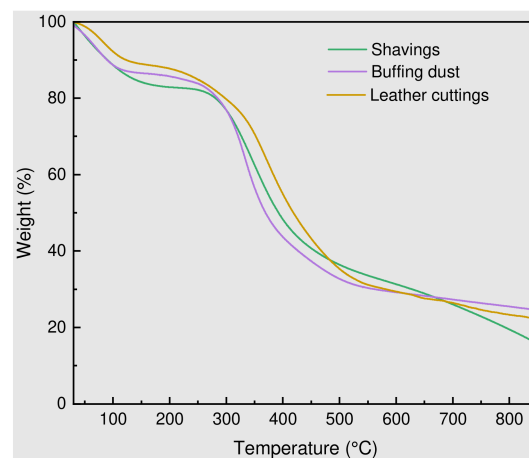


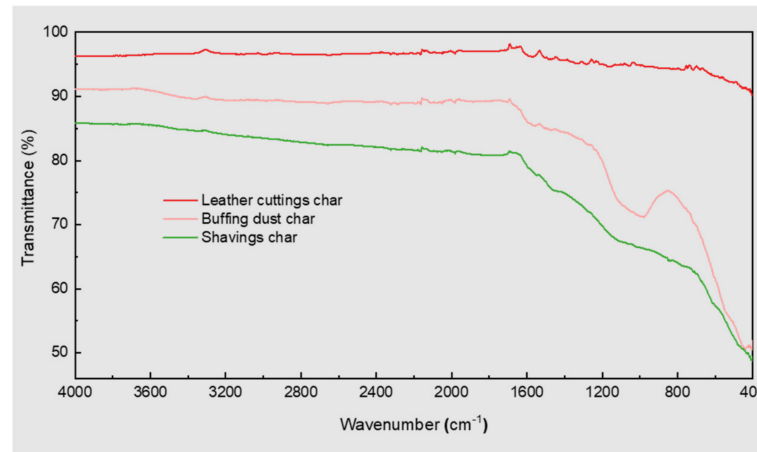
**Figure 8.** Thermogravimetric analysis of the Cr-containing leather wastes (Adapted from Nur-A-Tomal, et al. [7]. Reproduced with permission from Springer Nature).

### 3.3.1. Production of Char from Used Leather

Hard carbon (char) was produced using a horizontal tube furnace at a temperature of 800 °C in an Ar gas atmosphere [55]. The produced chars from leather wastes were further characterised using a macro combustion analyser. The chemical composition of the produced chars is reported in Table 3. It is obvious from the results that the produced chars are a good source of carbon. The content of carbon in the char from shavings, buffing dust, and leather cuttings are 50.0%, 39.0%, and 68.9%, respectively. Additionally, the chars contain a considerable amount of hydrogen, which could also aid the reduction of iron oxide [7]. The FTIR spectra of produced chars are shown in Figure 9. After charring at 800 °C, it was noticed that all functional groups had nearly disappeared. The FTIR spectra of the char showed a resemblance to the spectrum of graphite.

**Table 3.** Chemical composition of prepared char from leather wastes. (Adapted from Nur-A-Tomal, et al. [7]. Reproduced with permission from Springer Nature).

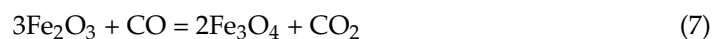
Element	Shavings Char	Buffing Dust Char	Leather Cuttings Char
Carbon (%)	50.0	39.0	68.9
Nitrogen (%)	11.4	7.1	7.5
Hydrogen (%)	2.5	1.1	2.4
Sulphur (%)	1.9	2.7	1.2

**Figure 9.** FTIR spectra of the char from Cr-containing leather waste samples (Adapted from Nur-A-Tomal, et al. [7]. Reproduced with permission from Springer Nature).

The produced chars from leather wastes were further characterised using a macro combustion analyser. The chemical composition of produced chars is reported in Table 3. It is obvious from the results that the produced chars are a good source of carbon [56,57]. The carbon content in the char from shavings, buffing dust, and leather cuttings were 50.0%, 39.0%, and 68.9%, respectively. Moreover, the chars also contain a substantial quantity of hydrogen, which could positively affect iron oxide reduction.

### 3.3.2. Char-Based Reduction of Iron Oxide ( $\text{Fe}_2\text{O}_3$ )

The chars produced from Cr-containing leather wastes were utilised to reduce iron oxide to prove their capability in ironmaking as an alternate source of carbon. Pellets were prepared from  $\text{Fe}_2\text{O}_3$  (purity 99%) and char powders by mix-agglomeration with a small quantity of water. The reduction experimentations were carried out using a horizontal tube furnace at a temperature of 1550 °C in an Ar gas atmosphere. The generated gas, such as CO,  $\text{CO}_2$ ,  $\text{CH}_4$ , and  $\text{H}_2$ , from the reduction reactions using an IR gas analyser, which is shown in Figure 10. Below are the reactions that normally happen during the reduction of iron oxide [7]:



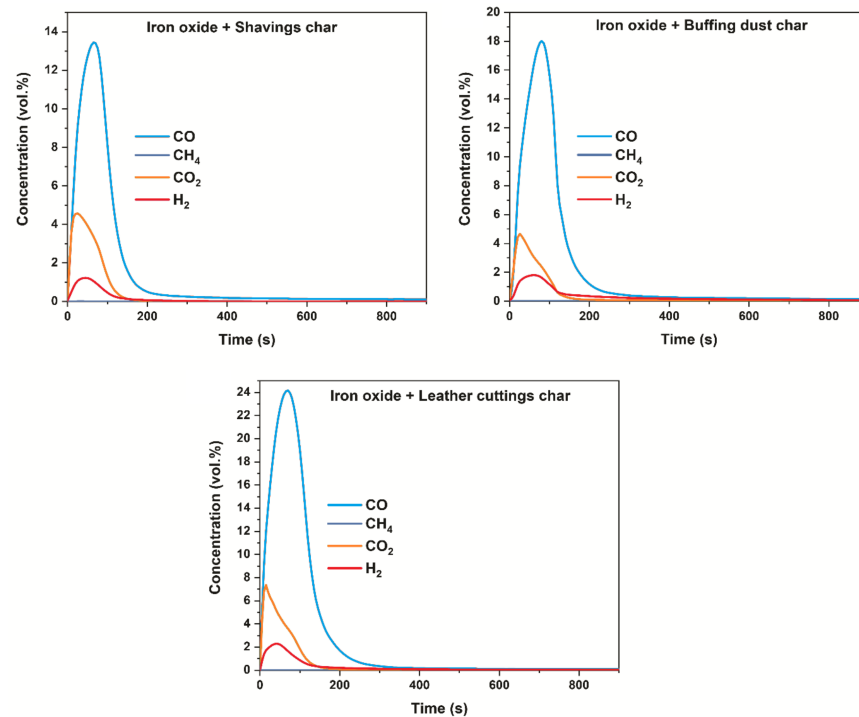


**Figure 10.** Off-gas produced during the reduction experiments using char produced from leather wastes (Adapted from Nur-A-Tomal, et al. [7]. Reproduced with permission from Springer Nature).

The generation of off-gases is highest for leather cuttings due to the high content of carbon, which holds the regeneration of the gas mix. The extent of reduction and oxygen removal rate was determined from the weight loss and off-gas analysis data, as illustrated in Figure 11. From Figure 11a, the leather waste that completes the reduction earlier can be summarised as leather cuttings > shavings > buffing dust. H<sub>2</sub> is believed to be an advanced reducing agent than CO and carbon. H<sub>2</sub> would have initiated the reduction reaction flourished by CO. This could be the reason for the earliest completion of the reduction process for the leather cuttings char because it contains comparatively high carbon content, even though it contains a comparable hydrogen content to that of shavings. At the subsequent reduction stage, the gasification of carbon by CO is vital to complete the reduction. The buffing dust char took a comparatively extended time owing to a lower amount of carbon.

The produced iron droplets were subject to elemental analyses using laser-induced breakdown spectroscopy (LIBS), which is summarised in Table 4. The LIBS results indicate that the produced droplets using all three chars contain about 99.7% Fe. In addition, the droplets contain a low quantity of C and Cr. The experimental results imply that the char from solid leather wastes can be used as a reductant for ironmaking.

**Table 4.** Elemental analysis of metal droplets produced from the reduction of iron (III) oxide and prepared chars from leather wastes using laser-induced breakdown spectroscopy (LIBS) [7].

Element	Concentration of Metals Produced Using		
	Shavings Char (%)	Buffing Dust Char (%)	Leather Cuttings Char (%)
Fe	99.70 ± 0.06	99.70 ± 0.05	99.7 ± 0.04
C	0.05 ± 0.02	0.03 ± 0.01	0.025 ± 0.01
Cr	0.12 ± 0.01	0.12 ± 0.12	0.024 ± 0.003
Mn	0.11 ± 0.02	0.10 ± 0.01	0.122 ± 0.01

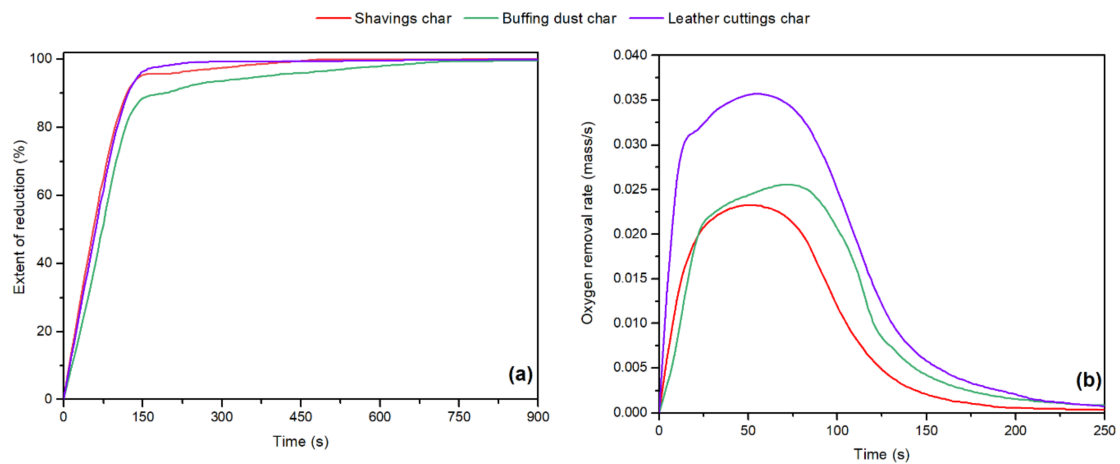


**Figure 11.** (a) Extent of reduction and (b) oxygen removal rate of iron oxide with the chars produced from chromium-containing leather wastes (Adapted from Nur-A-Tomal, et al. [7]). Reproduced with permission from Springer Nature).

### 3.4. Spent Coffee Grounds (SCGs)

For the application in sustainable ironmaking, SCGs were thermally transformed to T-SCGs (transformed-spent coffee grounds) under suitable conditions, as described in the subsequent sections [58]. The SCGs and T-SCGs were subjected to proximate and ultimate analyses, and the results are shown in Figure 12. Thermal transformation of SCGs led to devolatilisation as the volatile content of the SCGs is released by breaking of chemical bonds favoured at that temperature and, consequently, enhancing the solid carbon content [59,60].

Table 5 presents the ash composition of SCGs (analysed on an ashed basis, representing major oxide). Potassium oxide is one of the most prevalent compounds in the inorganic matter of biomasses and is highly concentrated in ash [61]. Alkali elements, such as sodium, potassium, and calcium, have a catalytic action that speeds up bond dissociation and the generation of smaller molecules during thermal transformation.

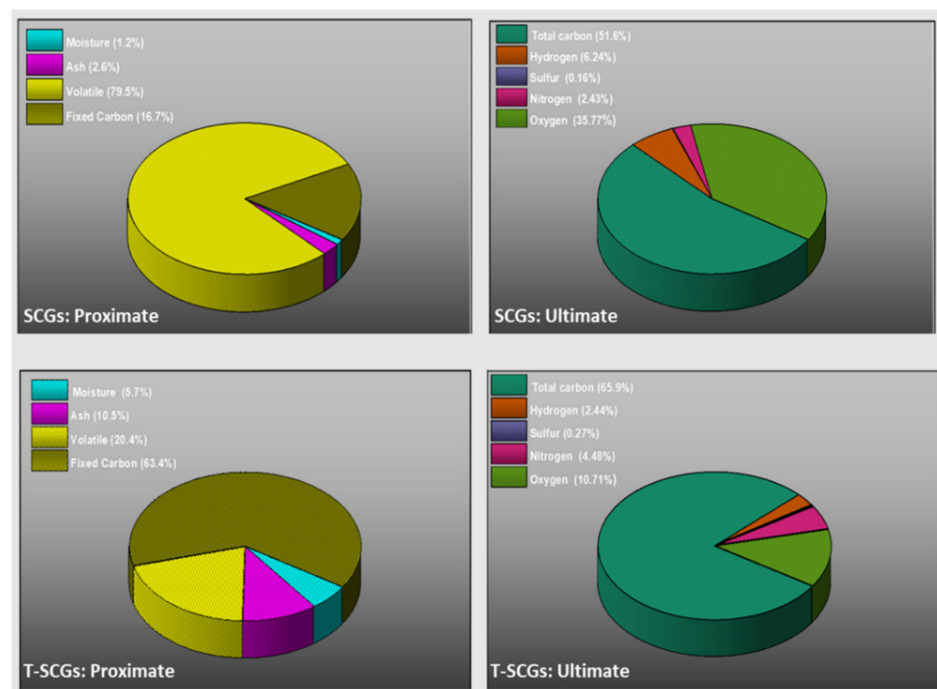


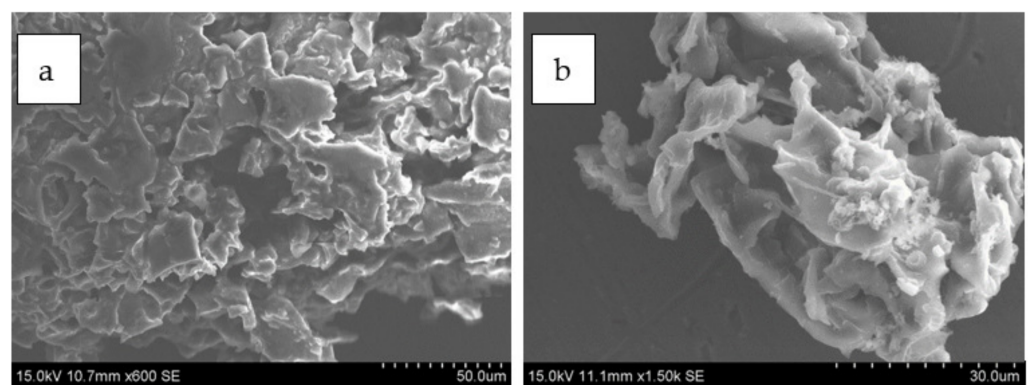
**Figure 12.** Proximate and ultimate analyses of SCGs and T-SCGs (Adapted from Biswal, et al. [58]). Reproduced with permission from Elsevier).

**Table 5.** Ash analysis of SCGs (Adapted from Biswal, et al. [58]. Reproduced with permission from Elsevier).

Oxides	SiO <sub>2</sub>	Al <sub>2</sub> O <sub>3</sub>	Fe <sub>2</sub> O <sub>3</sub>	Mn <sub>3</sub> O <sub>4</sub>	MgO	CaO	Na <sub>2</sub> O	K <sub>2</sub> O	P <sub>2</sub> O <sub>5</sub>	SO <sub>3</sub>
SCGs (weight %)	0.70	0.31	0.31	0.28	18.30	11.95	3.56	29.35	17.23	5.49

### 3.4.1. Formation of T-SCGs

To eliminate surface moisture, SCGs were dried in an electrically heated oven at 80 °C for 24 h. Alumina crucible containing 50 g of SCGs were heated for 30 min at 400 °C in a chamber furnace using Ar gas flowing at a rate of 3 L/min. The obtained product was named T-SCGs. The morphological analysis of the SCGs and the transformed product are shown in Figure 13.

**Figure 13.** SEM micrographs of spent (a) coffee grounds (SCGs) and (b) transformed-spent coffee grounds (T-SCGs).

### 3.4.2. Pellet Preparation

Three kinds of composite pellets (8–12 mm in diameter) were made by hand-rolling mixtures created with hematite powder (>99% purity) and carbonaceous material. The chemical compositions of the pellets complied with stoichiometric specifications. The pellets consisted of iron oxide combined with S.C.G.s, T-SCGs, and MC (metallurgical coke). Metallurgical coke was also used for the reduction study to compare the reduction efficiency of waste resources with that of conventional materials. Except for distilled water, no other special binder was employed to make the pellets. The green pellets were first air-dried for 16 h, then dried for another two hours in an electrically heated oven [58].

### 3.4.3. Heat Treatment of Pellets

The composite pellets were put into the high-temperature horizontal tube furnace in an alumina-based crucible that was placed atop a graphite rod. To prevent any thermal shock, the rod was kept in the furnace's cold zone for around 10 min. After that, it was gently moved into the hot zone (maintained at the desired temperature), which was then kept for 15 min. Before being eventually removed from the furnace set up, the rod was gently pushed back into the cold zone once more and held there for an additional 10 min. Ar gas was continuously purged into the furnace at a flow rate of 1 L/min [9,58].

### 3.4.4. Transformed-Spent Coffee Grounds (T-SCGs)-Based Hematite Reduction

The reduction of the pellets was carried out at temperatures of 1150, 1250, 1400, and 1550 °C, and the XRD analysis of the end-products was carried out and has been reported in previously published work [58]. The degree of reduction at each temperature (except for 1550 °C) was calculated based on Rietveld quantification of the XRD data, and the results are presented in Figure 14.

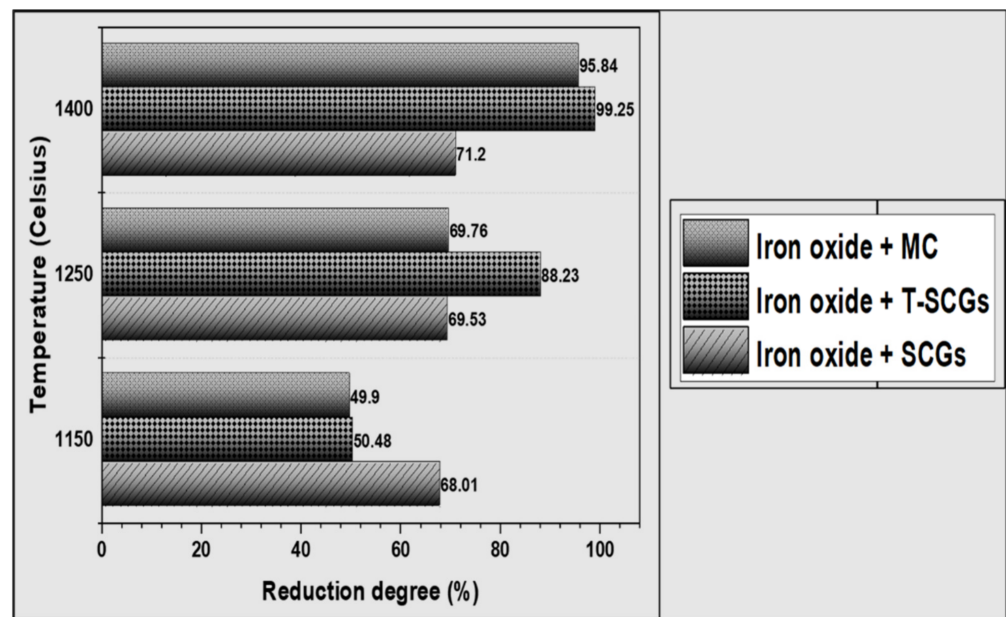


**Figure 14.** Degree of reduction of hematite-based pellets heat-treated at different temperatures (Adapted from Biswal, et al. [58]. Reproduced with permission from Elsevier).

It could be observed from the reduction degree calculations that the reduction performance of the pellet with SCGs was better at 1150 °C, but with the increase in temperature, T-SCGs reduction efficiency became better. It is interesting to note that the reduction performance of SCGs or T-SCGs was better than that of MC at a particular temperature. At isothermal reduction, hydrogen may initiate the process remarkably quickly, but as CO and CO<sub>2</sub> concentrations gradually rise, these gases obstruct hydrogen's access to reaction sites and lower the reduction rate [62–64]. However, once the secondary breakdown phase of the SCGs begins, the volume of CO, which is subsequently participating in the reduction reaction, increases while the volume percentage of hydrogen steadily decreases. Due to the low fixed carbon content of the SCGs (given in Figure 12) and the improper entrapment of the gas mix produced during the initial stage, the decrease in the subsequent stage of reduction would have been impacted. Using SCGs as a reduction agent produces a significant quantity of gas mix, which in turn creates the pores in the pellet, which ought to enhance the surface area of the solid-gas interfacial reaction. Tiny cracks are formed due to the pellet's increased porosity caused by the released volatiles. The gases in the mixture meant to participate in the reduction process can easily escape via these cracks in the atmosphere. Hence, even though the generation of the gas mix is vigorous, there is hardly any increase in the reduction degree with temperature [58].

In the case of T-SCGs, lower volatile matter makes it easier for hydrogen to access the reaction areas, and at a later stage, CO participates in the reduction reaction generated by the gasification process. Given that there is no surplus gas mix preventing access to reaction sites, it can be argued that the hydrogen in the T-SCGs participates in an efficient reduction atmosphere. Later, the solid carbon's behaviour (which is comparable to that of MC) plays a crucial part in strengthening the reduction process. In the literature, the reduction mechanism of iron oxide with MC has already been reported. Overall, T-SCGs exhibit more reduction than SCGs and MC, but it is possible that SCGs could achieve results that are equivalent to those of T-SCGs, provided the gas mix is properly trapped [9,58]. When used in the ferrous sector as a secondary carbon resource, SCGs—which are an everyday waste material—can reduce carbon emissions, energy requirements, and mining expenses. With the use of transformational technologies, the present ferrous industry may move towards sustainability for the economy and the environment by maximising the utilisation of waste products such as SCGs.

#### 4. Conclusions

The thermal transformation process boasts an attractive route for continuous material recycling for wastes that typically end up in landfills. The products obtained as a result of the thermal transformation processes of textile and leather wastes, automotive shredder residues (ASR), and spent coffee grounds (SCGs) have demonstrated remarkable attributes as activated carbon and reductants in metallurgical industries. These approaches, therefore, have significant potential for product development.

**Author Contributions:** S.H., C.W., S.B. and M.S.N.-A.-T.: Experiments, Formal analysis, writing: Original Draft, Review and Editing. S.U. and N.S.: Review and Editing. V.S. and F.P.: Conceptualisation, Formal analysis, writing: Review and Editing, Supervision, Project Administration, Funding Acquisition. All authors have read and agreed to the published version of the manuscript.

**Funding:** This research received no external funding.

**Data Availability Statement:** Data can be available upon request from the authors.

**Acknowledgments:** We gratefully acknowledge analytical support given by the Mark Wainwright Analytical Centre (MWAC), UNSW, Sydney, Australia.

**Conflicts of Interest:** The authors declare no conflict of interest.

#### References

1. Fiksel, J.; Lal, R. Transforming waste into resources for the Indian economy. *Environ. Dev.* **2018**, *26*, 123–128. [CrossRef]
2. Shen, L.; Worrell, E. Plastic recycling. In *Handbook of Recycling*; Elsevier: Amsterdam, The Netherlands, 2014; pp. 179–190.
3. Cossu, R.; Lai, T. Automotive shredder residue (ASR) management: An overview. *Waste Manag.* **2015**, *45*, 143–151. [CrossRef] [PubMed]
4. Hemati, S.; Hossain, R.; Sahajwalla, V. Selective thermal transformation of automotive shredder residues into high-value nano silicon carbide. *Nanomaterials* **2021**, *11*, 2781. [CrossRef] [PubMed]
5. Juanga-Labayen, J.P.; Labayen, I.V.; Yuan, Q. A review on textile recycling practices and challenges. *J. Text.* **2022**, *2*, 174–188. [CrossRef]
6. Chojnacka, K.; Skrzypczak, D.; Mikula, K.; Witek-Krowiak, A.; Izydorczyk, G.; Kuligowski, K.; Bandrów, P.; Kułazyński, M. Progress in sustainable technologies of leather wastes valorization as solutions for the circular economy. *J. Clean. Prod.* **2021**, *313*, 127902. [CrossRef]
7. Nur-A-Tomal, M.S.; Biswal, S.; Pahlevani, F.; Sahajwalla, V. Recycling tannery solid wastes as an alternative carbon resource for ironmaking. *J. Mater. Cycles Waste Manag.* **2022**, *24*, 2030–2040. [CrossRef]
8. McNutt, J. Spent coffee grounds: A review on current utilization. *J. Ind. Eng. Chem.* **2019**, *71*, 78–88. [CrossRef]
9. Biswal, S.; Pahlevani, F.; Sahajwalla, V. Synthesis of Value-Added Ferrous Material from Electric Arc Furnace (EAF) Slag and Spent Coffee Grounds. *JOM* **2021**, *73*, 1878–1888. [CrossRef]
10. Gordon, S.; Hsieh, Y.-I. *Cotton: Science and Technology*; Woodhead Publishing: Sawston, UK, 2006.
11. Macmillan, C.; Birke, H.; Bedon, F.; Pettolino, F. Lignin deposition in cotton cells—Where is the lignin. *J. Plant Biochem. Physiol.* **2013**, *1*, e106. [CrossRef]
12. Jody, B.; Daniels, E.; Duranceau, C.; Pomykala, J.; Spangenberg, J. End-of-Life Vehicle Recycling: State of the Art of Resource Recovery from Shredder Residue. 2010. Available online: <https://publications.anl.gov/anlpubs/2011/02/69114.pdf> (accessed on 27 November 2022).
13. GHK. A Study to Examine the Benefits of the End of Life Vehicles Directive and the Costs and Benefits of a Revision of the 2015 Targets for Recycling, Re-Use and Recovery under the ELV Directive. Final Report to DG Environment, Birmingham, USA. 2006, pp. 3–4. Available online: [https://ec.europa.eu/environment/pdf/waste/study/final\\_report.pdf](https://ec.europa.eu/environment/pdf/waste/study/final_report.pdf) (accessed on 27 November 2022).
14. Masilamani, D.; Srinivasan, V.; Ramachandran, R.K.; Gopinath, A.; Madhan, B.; Saravanan, P. Sustainable packaging materials from tannery trimming solid waste: A new paradigm in wealth from waste approaches. *J. Clean. Prod.* **2017**, *164*, 885–891. [CrossRef]
15. Famielec, S. Chromium concentrate recovery from solid tannery waste in a thermal process. *Materials* **2020**, *13*, 1533. [CrossRef]
16. Ridder, M. *Coffee Market Worldwide 2022: Report*; Statista Inc.: Hamburg, Germany, 2022; p. 36.
17. Cameron, A.O.M. *Sean Coffee 4 Planet Ark: Final Report for the City of Sydney*; 2015/199344; The Council of the City of Sydney: Sydney, Australia, 2016; p. 21.
18. Campos-Vega, R.; Loarca-Pina, G.; Vergara-Castañeda, H.A.; Oomah, B.D. Spent coffee grounds: A review on current research and future prospects. *Trends Food Sci. Technol.* **2015**, *45*, 24–36. [CrossRef]
19. Shukla, A.; Sharma, V.; Basak, S.; Ali, S.W. Sodium lignin sulfonate: A bio-macromolecule for making fire retardant cotton fabric. *Cellulose* **2019**, *26*, 8191–8208. [CrossRef]

20. Kundu, C.K.; Li, Z.; Song, L.; Hu, Y. An overview of fire retardant treatments for synthetic textiles: From traditional approaches to recent applications. *Eur. Polym. J.* **2020**, *137*, 109911. [CrossRef]
21. Nilsson, D.; Holmstedt, G. *Kompedium i Aktiva System-Detektion*; LUTVDG/TVBB-7030-SE; Lund University: Lund, Sweden, 2008; Volume 7030, p. 81.
22. Li, P.; Wang, B.; Xu, Y.-J.; Jiang, Z.; Dong, C.; Liu, Y.; Zhu, P. Ecofriendly flame-retardant cotton fabrics: Preparation, flame retardancy, thermal degradation properties, and mechanism. *ACS Sustain. Chem.* **2019**, *7*, 19246–19256. [CrossRef]
23. Hsieh, Y.-L. Chemical Structure and Properties of Cotton. In *Cotton: Science and Technology*; Gordon, S., Hsieh, Y.L., Eds.; Woodhead Publishing Limited: Sawston, UK; CRC Press: Boca Raton, FL, USA, 2007; pp. 3–34.
24. Williams, P.T.; Reed, A.R. High grade activated carbon matting derived from the chemical activation and pyrolysis of natural fibre textile waste. *J. Anal. Appl. Pyrolysis* **2004**, *71*, 971–986. [CrossRef]
25. Wesley, C.; Pahlevani, F.; Nur-A-Tomal, S.; Biswal, S.; Sahajwalla, V. An investigation into the minimum energy requirements for transforming end-of-life cotton textiles into carbon fibre in an Australian context. *Resour. Conserv. Recycl. Adv.* **2023**, *17*, 200123. [CrossRef]
26. Jagdale, P.; Nair, J.R.; Khan, A.; Armandi, M.; Meligrana, G.; Hernandez, F.R.; Rusakova, I.; Piatti, E.; Rovere, M.; Tagliaferro, A. Waste to life: Low-cost, self-standing, 2D carbon fiber green Li-ion battery anode made from end-of-life cotton textile. *Electrochim. Acta* **2021**, *368*, 137644. [CrossRef]
27. DeSilva, F.J. Activated Carbon Filtration. *Water Quality Products Magazine*. 2000. Available online: <https://h2oblogged.files.wordpress.com/2010/05/activated20carbon20filtration.pdf> (accessed on 27 November 2022).
28. Khayyam Nekouei, R.; Mofarah, S.S.; Maroufi, S.; Wang, W.; Mansuri, I.; Sahajwalla, V. Unraveling the Role of Oxides in Electrochemical Performance of Activated Carbons for High Voltage Symmetric Electric Double-Layer Capacitors. *Adv. Energy Sustain. Res.* **2022**, *3*, 2100130. [CrossRef]
29. Ahammad, A.S.; Pal, P.R.; Shah, S.S.; Islam, T.; Hasan, M.M.; Qasem, M.A.A.; Odhikari, N.; Sarker, S.; Kim, D.M.; Aziz, M.A. Activated jute carbon paste screen-printed FTO electrodes for nonenzymatic amperometric determination of nitrite. *J. Electroanal. Chem.* **2019**, *832*, 368–379. [CrossRef]
30. Buekens, A.; Zhou, X. Recycling plastics from automotive shredder residues: A review. *J. Mater. Cycles Waste Manag.* **2014**, *16*, 398–414. [CrossRef]
31. Joung, H.-T.; Cho, S.-J.; Seo, Y.-C.; Kim, W.-H. Status of recycling end-of-life vehicles and efforts to reduce automobile shredder residues in Korea. *J. Mater. Cycles Waste Manag.* **2007**, *9*, 159–166. [CrossRef]
32. Kim, K.-H.; Joung, H.-T.; Nam, H.; Seo, Y.-C.; Hong, J.H.; Yoo, T.-W.; Lim, B.-S.; Park, J.-H. Management status of end-of-life vehicles and characteristics of automobile shredder residues in Korea. *Waste Manag.* **2004**, *24*, 533–540. [CrossRef] [PubMed]
33. Mark, F.E. *Del Reciclado a la Energía*. In Proceedings of the Conferencia Internacional Sobre Innovación em la Valorización de los Residuos Plásticos, Madrid, Spain; 2000.
34. Mayyas, M.; Pahlevani, F.; Handoko, W.; Sahajwalla, V. Preliminary investigation on the thermal conversion of automotive shredder residue into value-added products: Graphitic carbon and nano-ceramics. *Waste Manag.* **2016**, *50*, 173–183. [CrossRef] [PubMed]
35. Gotsis, A.; Zeevenhoven, B.; Hogt, A. The effect of long chain branching on the processability of polypropylene in thermoforming. *J. Polym. Eng. Sci.* **2004**, *44*, 973–982. [CrossRef]
36. Cabrera, N.; Alcock, B.; Loos, J.; Peijs, T. Processing of all-polypropylene composites for ultimate recyclability. *Proc. Inst. Mech. Eng. Part L J. Mater. Des. Appl.* **2004**, *218*, 145–155. [CrossRef]
37. Vermeulen, I.; Van Caneghem, J.; Block, C.; Baeyens, J.; Vandecasteele, C. Automotive shredder residue (ASR): Reviewing its production from end-of-life vehicles (ELVs) and its recycling, energy or chemicals' valorisation. *J. Hazard. Mater.* **2011**, *190*, 8–27. [CrossRef]
38. Al-Salem, S.; Lettieri, P.; Baeyens, J. Recycling and recovery routes of plastic solid waste (PSW): A review. *Waste Manag.* **2009**, *29*, 2625–2643. [CrossRef]
39. Al-Salem, S.; Lettieri, P.; Baeyens, J. The valorization of plastic solid waste (PSW) by primary to quaternary routes: From re-use to energy and chemicals. *Prog. Energy Combust. Sci.* **2010**, *36*, 103–129. [CrossRef]
40. Brems, A.; Baeyens, J.; Vandecasteele, C.; Dewil, R. Polymeric cracking of waste polyethylene terephthalate to chemicals and energy. *J. Air Waste Manag. Assoc.* **2011**, *61*, 721–731. [CrossRef]
41. De Marco, I.; Caballero, B.; Chomón, M.; Laresgoiti, M.; Torres, A.; Fernández, G.; Arnaiz, S. Pyrolysis of electrical and electronic wastes. *J. Anal. Appl. Pyrolysis* **2008**, *82*, 179–183. [CrossRef]
42. Maroufi, S.; Mayyas, M.; Sahajwalla, V. Novel synthesis of silicon carbide nanowires from e-waste. *ACS Sustain. Chem. Eng.* **2017**, *5*, 4171–4178. [CrossRef]
43. Wang, L.; Cheng, Q.; Qin, H.; Li, Z.; Lou, Z.; Lu, J.; Zhang, J.; Zhou, Q. Synthesis of silicon carbide nanocrystals from waste polytetrafluoroethylene. *Dalton Trans.* **2017**, *46*, 2756–2759. [CrossRef] [PubMed]
44. Farzana, R.; Rajarao, R.; Sahajwalla, V. Characteristics of waste automotive glasses as silica resource in ferrosilicon synthesis. *Waste Manag. Res.* **2016**, *34*, 113–121. [CrossRef] [PubMed]
45. Maroufi, S.; Mayyas, M.; Sahajwalla, V. Waste materials conversion into mesoporous silicon carbide nanoceramics: Nanofibre/particle mixture. *J. Clean. Prod.* **2017**, *157*, 213–221. [CrossRef]

46. An, Z.; Wang, H.; Zhu, C.; Cao, H.; Xue, J. Synthesis and formation mechanism of porous silicon carbide stacked by nanoparticles from precipitated silica/glucose composites. *J. Mater. Sci.* **2019**, *54*, 2787–2795. [[CrossRef](#)]
47. Ahmed, S.; Fatema-Tuj-Zohra; Khan, M.S.H.; Hashem, M.A. Chromium from tannery waste in poultry feed: A potential cradle to transport human food chain. *Cogent Environ. Sci.* **2017**, *3*, 1312767. [[CrossRef](#)]
48. Ravindranath, E.; Chitra, K.; Porselvam, S.; Srinivasan, S.; Suthanthararajan, R. Green energy from the combined treatment of liquid and solid waste from the tanning industry using an upflow anaerobic sludge blanket reactor. *J. Energy Fuels* **2015**, *29*, 1892–1898. [[CrossRef](#)]
49. Covington, A.D.; Wise, W.R. *Tanning Chemistry: The Science of Leather*, 2nd ed.; Royal Society of Chemistry: London, UK, 2020.
50. Vyskočilová, G.; Ebersbach, M.; Kopecká, R.; Prokeš, L.; Příhoda, J. Model study of the leather degradation by oxidation and hydrolysis. *Herit. Sci.* **2019**, *7*, 1–13. [[CrossRef](#)]
51. Mohamed, O.A.; El Sayed, N.H.; Abdelhakim, A.A. Preparation and characterization of polyamide-leather wastes polymer composites. *J. Appl. Polym. Sci.* **2010**, *118*, 446–451. [[CrossRef](#)]
52. Liu, J.; Luo, L.; Zhang, Z.; Hu, Y.; Wang, F.; Li, X.; Tang, K. A combined kinetic study on the pyrolysis of chrome shavings by thermogravimetry. *Carbon Resour. Convers.* **2020**, *3*, 156–163. [[CrossRef](#)]
53. Cardona, N.; Velásquez, S.; Giraldo, D. Characterization of Leather Wastes from Chrome Tanning and its Effect as Filler on the Rheometric Properties of Natural Rubber Compounds. *J. Polym. Environ.* **2017**, *25*, 1190–1197. [[CrossRef](#)]
54. Liu, J.; Luo, L.; Hu, Y.; Wang, F.; Zheng, X.; Tang, K. Kinetics and mechanism of thermal degradation of vegetable-tanned leather fiber. *J. Leather Sci. Eng.* **2019**, *1*, 1–13. [[CrossRef](#)]
55. Li, S.; Wang, H.; Chen, C.; Li, X.; Deng, Q.; Gong, M.; Li, D. Size effect of charcoal particles on the properties of bamboo charcoal/ultra-high molecular weight polyethylene composites. *J. Appl. Polym. Sci.* **2017**, *134*, 45530. [[CrossRef](#)]
56. Van Rensburg, M.L.; Nkomo, S.p.L.; Mkhize, N.M. Characterization and pyrolysis of post-consumer leather shoe waste for the recovery of valuable chemicals. *Multidiscip. J. Waste Resour. Residues* **2021**, *92*. [[CrossRef](#)]
57. Yılmaz, O.; Cem Kantarli, I.; Yuksel, M.; Saglam, M.; Yanik, J. Conversion of leather wastes to useful products. *Resour. Conserv. Recycl.* **2007**, *49*, 436–448. [[CrossRef](#)]
58. Biswal, S.; Pahlevani, F.; Bhattacharyya, S.K.; Sahajwalla, V. A novel reforming approach of utilizing spent coffee grounds to produce iron. *Resour. Conserv. Recycl.* **2020**, *163*, 105067. [[CrossRef](#)]
59. Colantoni, A.; Paris, E.; Bianchini, L.; Ferri, S.; Marcantonio, V.; Carnevale, M.; Palma, A.; Civitarese, V.; Gallucci, F. Spent coffee ground characterization, pelletization test and emissions assessment in the combustion process. *Sci. Rep.* **2021**, *11*, 1–14. [[CrossRef](#)]
60. Pujol, D.; Liu, C.; Gominho, J.; Olivella, M.À.; Fiol, N.; Villaescusa, I.; Pereira, H. The chemical composition of exhausted coffee waste. *Ind. Crops Prod.* **2013**, *50*, 423–429. [[CrossRef](#)]
61. Ballesteros, L.F.; Teixeira, J.A.; Mussatto, S.I. Chemical, functional, and structural properties of spent coffee grounds and coffee silverskin. *Food Bioprocess Technol.* **2014**, *7*, 3493–3503. [[CrossRef](#)]
62. Bonalde, A.; Henriquez, A.; Manrique, M. Kinetic analysis of the iron oxide reduction using hydrogen-carbon monoxide mixtures as reducing agent. *ISIJ Int.* **2005**, *45*, 1255–1260. [[CrossRef](#)]
63. Guo, D.; Hu, M.; Pu, C.; Xiao, B.; Hu, Z.; Liu, S.; Wang, X.; Zhu, X. Kinetics and mechanisms of direct reduction of iron ore-biomass composite pellets with hydrogen gas. *Int. J. Hydrogen Energy* **2015**, *40*, 4733–4740. [[CrossRef](#)]
64. Luo, S.; Yi, C.; Zhou, Y. Direct reduction of mixed biomass-Fe<sub>2</sub>O<sub>3</sub> briquettes using biomass-generated syngas. *Renew. Energy* **2011**, *36*, 3332–3336. [[CrossRef](#)]

**Disclaimer/Publisher’s Note:** The statements, opinions and data contained in all publications are solely those of the individual author(s) and contributor(s) and not of MDPI and/or the editor(s). MDPI and/or the editor(s) disclaim responsibility for any injury to people or property resulting from any ideas, methods, instructions or products referred to in the content.